Interpolated gain-scheduled controllers for an Over-head Crane

Keivan Zavari, Goele Pipeleers and Jan Swevers
Department of Mechanical Engineering, Katholieke Universiteit Leuven, Belgium.
Email: keivan.zavari@mech.kuleuven.be

***Abstract*—This paper presents a practical way to design gain-scheduled controllers for linear parameter varying (LPV) systems. An existing state-space model interpolation method for LPV systems is exploited in order to derive the desired controller. The interpolation requires designing local LTI controllers for local working conditions of the system, which is performed using a multi-objective $\mathcal{H}_\infty$ approach. To simplify the weighting function design, the $\mathcal{H}_\infty$ objective is broken apart into different $\mathcal{H}_\infty$ design objectives and constraints, each related to various input-output combinations. The developed LPV control design approach is illustrated on an over-head crane system.**

I. Introduction

To describe the dynamics of systems affected by time-varying parameters or nonlinearities, Linear Parameter Varying (LPV) models act as a powerful tool by representing systems in terms of linear models affected by time varying parameters called the scheduling parameters. The scheduling parameters are usually unknown a priori but assumed to be measured or estimated in real-time.

There is a continuing effort to design LPV controllers, scheduled as a function of the varying parameters, in order to achieve higher performance while still guaranteeing stability for all possible parameter variations [1]. One method to achieve this, is synthesizing the controller directly from the LPV model, which is commonly referred to as the LPV gain-scheduling method. In order to obtain this controller, there are several techniques built upon Lyapunov functions or small-gain approaches [1]. Another method is to compute a gain-scheduled controller from a set of local LTI controllers designed for different local working conditions of the LPV system. While this method cannot provide a guarantee for stability and performance, it is generally considered more practical and intuitive.

The method presented in this paper belongs to the second category and it consists of the following steps. First, a family of linear time-invariant (LTI) models is determined by selecting different local operating conditions of the system. Second, local controllers for each one of the local LTI models are designed. Third, based on the values of the parameters, the local controllers are scheduled using some interpolation method (see e.g. [2]). Our approach utilizes a recently developed method for LPV modeling called state-space model interpolation of local estimates (SMILE) [3]. Since the stability and performance for the whole range of variation cannot be guaranteed, the final step is to validate the closed-loop stability and performance e.g. through simulations.

In order to synthesize local the LTI controllers, this paper proposes a multi-objective $\mathcal{H}_\infty$ control approach. In spite of the theoretical maturity of classical $\mathcal{H}_\infty$ control [4], it is generally not acknowledged as an easy and intuitive control design strategy. This is primarily due to the fact that a closed-loop $\mathcal{H}_\infty$ norm itself has limited practical value and invokes the addition of weighting functions. We propose to facilitate the weighting function design by solving the multi-objective control problem comprising multiple separate $\mathcal{H}_\infty$ norms on closed-loop subsystems. This results in a more intuitive LTI control problem formulation compared to classical $\mathcal{H}_\infty$ design since it allows distinguishing between design objectives and constraints, and imposing them on selected closed-loop subsystems. The difficulty arising from this approach is the non-convexity of the problem, and hence we resort to the Lyapunov shaping paradigm, which is a convex but conservative solution strategy for general multi-objective control problems [5].

This paper is organized as follows: Section II describes the LTI control problem formulation together with the numerical solution strategy. In Section III the interpolation approach to derive gain-scheduled controller from local LTI controllers is described, while Section IV demonstrates its potential on an over-head crane simulation example. Conclusions and final remarks follow in Section V.

Notation The set of integers is indicated by $\mathbf{N}$, and $\mathbf{S}_n$ is the set of real symmetric $n \times n$ matrices. For a matrix $X \in \mathbf{S}_n$, the inequalities $X \prec 0$ and $X \succ 0$ mean X is negative definite, respectively positive definite. Throughout the paper, the notation

$$H = \left[\begin{array}{c|c} A & B \\ \hline C & D \end{array}\right]$$

is used to indicate the state-space model system H:

$$H : \begin{cases} \delta x &= Ax + Bw \\ z &= Cx + Dw \end{cases},$$

where δ denotes the one-shift-advance operator for the discrete-time case or the differentiator for continuous time.

Sans-Serif font e.g. A_ℓ is used to denote local LTI models and their system matrices and to distinguish them from the other matrices which are shown using Standard font e.g. A_i.

II. Multi-$\mathcal{H}_\infty$ Controller Design

Section II-A presents the control problem formulation, while Section II-B describes the numerical solution of the resulting multi-objective control problem.

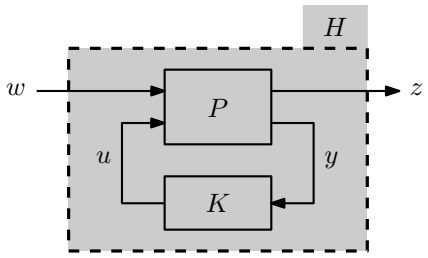

Fig. 1. General control configuration for the multi-$\mathcal{H}_\infty$ controller design. The $\mathcal{H}_\infty$ norms are imposed on subsystems $H_{(i,j)}$ for $(i,j) \in \mathcal{I}$.

A. Problem Formulation

We consider a multi-objective control problem involving various $\mathcal{H}_\infty$ specifications on selected closed-loop subsystems. The problem is formulated in the general control configuration as depicted in Figure 1. The system P denotes the generalized plant and includes the weighting functions, K is the controller to be designed and H denotes the closed-loop system. The signals u and y respectively correspond to the control signal and the measured output, while the $\mathcal{H}_\infty$ design specifications are formulated by means of the exogenous input w and the regulated output z. The considered $\mathcal{H}_\infty$-norms are labeled by the index $i \in \mathcal{I} \subset \mathbf{N}$, and the i^{th} $\mathcal{H}_\infty$ norm is imposed on closed-loop subsystem H_i of the following form:

$$H_i = E_i H F_i \,, \tag{1}$$

where the matrices E_i, F_i select the appropriate input/output channels. The set $\mathcal{I} = \mathcal{I}_\mathrm{c} \cup \mathcal{I}_\mathrm{o}$, where $\mathcal{I}_\mathrm{c}$ groups the indices relating to design constraints, while $\mathcal{I}_\mathrm{o}$ relates to the design objectives. The order of P is denoted by n, and only the full-order controller design is considered, that is: the controller K is parameterized as a dynamical system of the same order n as the generalized plant P. The controller parameters are computed as the optimal solution of the following problem:

$$\begin{aligned}
\underset{K \in \mathcal{S}_n, \gamma_i}{\text{minimize}} \quad & \sum_{i \in \mathcal{I}_\mathrm{o}} \beta_i \gamma_i && && \text{(2a)}\\
\text{subject to} \quad & \|H_i\|_\infty < \gamma_i \,, && \forall i \in \mathcal{I} && \text{(2b)}\\
& \gamma_i = 1 \,, && \forall i \in \mathcal{I}_\mathrm{c} \,, && \text{(2c)}
\end{aligned}$$

where $\mathcal{S}_n$ denotes the set of stabilizing controllers of order n. In the sequel, the closed-loop system H is indicated as:

$$H = \left[\begin{array}{c|c} A & B \\ \hline C & D \end{array}\right]. \tag{3}$$

For reasons of conciseness the dependency of A, B, C, D on the controller K is not mentioned explicitly. The matrices B_i, C_i and D_i are defined as the IO combination state-space matrices:

$$B_i = B F_i \,, \quad C_i = E_i C \,, \quad D_i = E_i D F_i \,.$$

B. Numerical Solution

The synthesis problem (2) is a multi-objective control problem and to date, no exact convex reformulation of such problems exists. Here, the problem is solved using the Lyapunov shaping paradigm [5], a convex, yet conservative solution approach for general multi-objective control problems. For a discrete-time control problem, this approach relies on the following, conservative, reformulation of (2):

$$\begin{aligned}
\text{minimize} \quad & \sum_{i \in \mathcal{I}_\mathrm{o}} \beta_i \gamma_i^2 && && \text{(4a)}\\
\text{subject to} \quad & Q \succ 0 && && \text{(4b)}\\
& \begin{bmatrix} A^T Q A - Q & A^T Q B_i & C_i^T \\ B_i^T Q A & B_i^T Q B_i - \gamma_i I & D_i^T \\ C_i & D_i & -\gamma_i I \end{bmatrix} \prec 0 \,, && \forall i \in \mathcal{I} && \text{(4c)}\\
& \gamma_i = 1 \,, && \forall i \in \mathcal{I}_\mathrm{c} \,, && \text{(4d)}
\end{aligned}$$

where the optimization variables are the Lyapunov matrix $Q \in \mathbf{S}_{2n}$, $K \in \mathcal{S}_n$ and γ_i. The corresponding reformulation for the continuous-time case can be found in [5]. The conservatism of the Lyapunov shaping paradigm stems from the fact that the same Lyapunov matrix Q is used in all the matrix inequalities. Problem (4) is transformed into a convex problem by means of the nonlinear change of controller variables presented in [6], [5].

III. Interpolation of local controllers

This section briefly presents the SMILE interpolation technique proposed in [3] for modeling MIMO LPV systems. This technique is based on the interpolation of state-space models that are estimated for m fixed operating conditions of the system and it works for both continuous- and discrete-time systems.

The aim of the interpolation is to derive the state-space model

$$T(\alpha) = \left[\begin{array}{c|c} A(\alpha) & B(\alpha) \\ \hline C(\alpha) & D(\alpha) \end{array}\right], \tag{5}$$

where the state-space matrices are parametrized using a polynomial dependency of degree $g < m$ on the scheduling parameter α which takes values in the unit-simplex Λ. Thus

$$A(\alpha) = \sum_{k=0}^{g} \alpha^k A_k, \tag{6}$$

and the matrices $B(\alpha), C(\alpha), D(\alpha)$ can be written similarly.

The local models are derived for different constant values of the scheduling parameters and the interpolation problem is formulated as a linear least square problem that can be efficiently solved.

This interpolation approach consists of the following three steps. First, a set of local LTI state-space models are obtained for m fixed-operating conditions. The second step is transforming all local models to a consistent representation. In literature several approaches are proposed to do this transformation. The method used in [3] sorts the poles and zeros

of the local models to derive the consistent models. The first two steps are presented in section III-A.

In the third step, a parameter dependent model is computed by interpolating the set of consistent LTI models. Typical choices for parametrization are affine, polytopic, polynomial or homogeneous polynomial parametrization. This step is described in section III-B.

A. Construction of consistent local MIMO models

Since different techniques can be used to obtain local LTI models and since the state-space representation is not unique, it is not guaranteed that the LTI models are represented in a consistent state-space form. Hence the local models

$$\widetilde{\mathsf{T}}_\ell = \left[\begin{array}{c|c} \widetilde{\mathsf{A}}_\ell & \widetilde{\mathsf{B}}_\ell \\ \hline \widetilde{\mathsf{C}}_\ell & \widetilde{\mathsf{D}}_\ell \end{array}\right], \tag{7}$$

where $\ell = 1, \ldots, m$ denotes the different local conditions, cannot be readily interpolated.

Therefore a similarity transformation matrix is needed to transform each local model $\widetilde{\mathsf{T}}_\ell$ to the consistent representation T_ℓ. Constructing the consistent MIMO models needs different steps. First an IO combination of the original system is chosen and then a consistent SISO model of this selected IO combination is constructed by sorting the poles and zeros. In the next step the similarity transformation matrix is derived that takes the original SISO model to the constructed consistent one. Afterwards this transformation matrix is also applied to the other IO combinations of the MIMO model. These steps are described more in details below.

1) Choice of IO combination : SMILE technique for MIMO systems consists of an extra step of choosing one IO combination (i, j). Considering this IO combination $\widetilde{\mathsf{T}}_{\ell,(i,j)}$ from the original local MIMO LTI models $\widetilde{\mathsf{T}}_\ell$ enables the user to sort the poles and the zeros. It is clear that for a local MIMO LTI model with r inputs and s outputs, there are $r.s$ possible combinations. However, the choice of the IO combination is limited since all resulting local SISO LTI models $\widetilde{\mathsf{T}}_{\ell,(i,j)}$ for $\ell = 1, \ldots, m$ need: 1) to be controllable (or observable) and 2) to have the same number of zeros.

2) Calculating and Sorting Poles and Zeros : To construct the consistent $\mathsf{T}_{\ell,(i,j)}$ for m local SISO models, the next step is calculating and sorting the poles and zeros. For a minimal state-space model, the poles are readily obtained as the eigenvalues of $\widetilde{\mathsf{A}}_\ell$. The zeros are also computed by solving a generalized eigenvalue problem that involves $\widetilde{\mathsf{A}}_\ell, \widetilde{\mathsf{B}}_{\ell,i}, \widetilde{\mathsf{C}}_{\ell,j}$ and $\widetilde{\mathsf{D}}_{\ell,(i,j)}$ (see [3] for more details).

3) Constructing consistent SISO models : The next step is to transform all the local SISO models $\widetilde{\mathsf{T}}_{\ell,(i,j)}$ to a new state-space form such that they are defined with respect to the same state-space representation basis. In order to achieve this, the original SISO models are represented as a gain $\mathsf{k}_{\ell,(i,j)}$ multiplied with the state-space series connection of first and second order state-space submodels. This can be written as:

$$\mathsf{T}_{\ell,(i,j)} = \mathsf{k}_{\ell,(i,j)} \prod_{\tau=1}^{\tau_1+\tau_2} \mathsf{T}^\tau_{\ell,(i,j)}, \tag{8}$$

with

$$\mathsf{T}^\tau_{\ell,(i,j)} = \left[\begin{array}{c|c} \mathsf{A}^\tau_\ell & \mathsf{B}^\tau_\ell \\ \hline \mathsf{C}^\tau_\ell & \mathsf{D}^\tau_\ell \end{array}\right], \tag{9}$$

where τ_1 is the number of first-order and τ_2 is the number of second-order submodels. All SISO submodels are chosen to have the same number of τ_1 and τ_2. The type-1 model can have either 0 or 1 zero and a type-2 model can have 0,1 or 2 zeros. It is worth mentioning that $\mathsf{k}_{\ell,(i,j)}$ denotes the gain associated with the zero-pole-gain factorization of the model and not the DC gain.

4) Calculating the similarity transformation : Once the consistent SISO models are calculated, it is straightforward to compute the unique similarity transformation matrix from $\widetilde{\mathsf{T}}_{\ell,(i,j)}$ to the consistent local SISO model $\mathsf{T}_{\ell,(i,j)}$ for each ℓ. When the similarity transformations are calculated for all local models $\ell = 1, \ldots, m$, they are applied to the original local MIMO model $\widetilde{\mathsf{T}}_\ell$ to obtain the consistent local MIMO models T_ℓ.

B. Interpolation and optimization

The next and the final step is the interpolation of the local models by the MIMO LPV model and it is done by solving an optimization problem to find the unknown parameters A_k, B_k, C_k, D_k of interpolating model (5). In [3] the following linear least squares cost function is considered:

$$\begin{aligned} \mathbf{E} = \sum_{\ell=1}^{m} \Big\{ & \big\| \sum_k \alpha^k_\ell A_k - \mathsf{A}_\ell \big\|^2_F + \big\| \sum_k \alpha^k_\ell B_k - \mathsf{B}_\ell \big\|^2_F \\ & + \big\| \sum_k \alpha^k_\ell C_k - \mathsf{C}_\ell \big\|^2_F + \big\| \sum_k \alpha^k_\ell D_k - \mathsf{D}_\ell \big\|^2_F \Big\} \end{aligned} \tag{10}$$

where $\|.\|_F$ is the Frobenius norm of a matrix. If q is the vector of variables containing all the elements of the unknown matrices A_k, B_k, C_k, D_k, then the cost function can be written as $\mathbf{E} = \|F(q)\|^2_2$ which is a linear least squares problem and can be solved efficiently.

IV. Numerical Illustration

To illustrate the potential of the proposed controller design strategy, it is applied to investigate gain-scheduling controller design for an over-head crane. Section IV-A describes the model of the over-head crane, while Section IV-B formulates the corresponding control problem for fixed values of the rope length. The different steps to derive the gain-scheduled controller are described in Section IV-C. Finally Section IV-D validates the obtained controller on the simulation model.

A. System Model

The over-head crane system, schematically outlined in Figure 2, consists of a cart to which a mass is attached via a rope. The rope has a variable length $L = [0.35, 0.75]$ m. The cart position, mass position and swing angle are indicated by x_c,

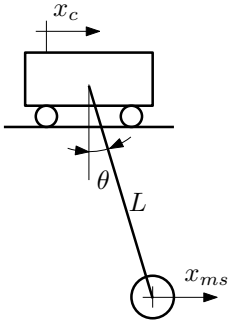

Fig. 2. Schematic outline of the over-head crane.

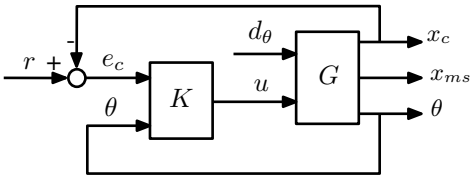

Fig. 3. Control configuration used for the over-head crane.

x_{ms} and θ, respectively. We assume that the cart is perfectly velocity controlled, such that $\dot{x}_c$ equals the external control input u:

$$\frac{x_c}{u} = \frac{1}{s}\,. \tag{11a}$$

In addition, the swing angle θ is assumed to be small such that the swing angle dynamics may by approximated to be linear time invariant:

$$\frac{\theta}{x_c} = \frac{-s^2}{s^2 L + g}\,, \tag{11b}$$

and the mass position $x_{ms} = x_c + L\theta$. For $L = 0.45$ m the corresponding undamped natural eigenfrequency equals $f_n = 0.74$ Hz. Both x_c and θ are measured by an encoder.

The over-head crane is controlled according to the configuration outlined in Figure 3. The system G represents the over-head crane and is governed by (11) with scheduling parameter L. The disturbance input d_θ is also added to the model such that the system response to an impulse in d_θ corresponds to the autonomous response from an initial swing angle θ_0.

B. Control Problem Formulation

In this section the control problem is formulated for a fixed rope length L_ℓ and the controller K_ℓ represents the controller K designed for this length. The controllers K_ℓ have two goals, make the load follow the reference command r for all the values of L_ℓ, and reject the disturbances on the angle. To this end, all measured signals are fed back to the controller:

$$y = \begin{bmatrix} r - x_c \\ \theta \end{bmatrix} = \begin{bmatrix} e_c \\ \theta \end{bmatrix}\,.$$

Superior load tracking requires a controller that does not excite the system's resonance and hence, has an antiresonance at the eigenfrequency f_n. However, such a controller cannot compensate load swinging due to an initial angle deviation, as this compensation requires an harmonic control signal with frequency f_n. Consequently, load tracking and angle disturbance rejection are conflicting performance specifications in the controller design. This trade-off is treated with the help of the control strategy proposed in Section II. To this end, both specifications are quantified in terms of a weighted closed-loop $\mathcal{H}_\infty$ norm. Load tracking is quantified by $\gamma_e = \|W_e H_{r,e_{ms}}\|_\infty$ where $H_{r,e_{ms}}$ denotes the closed-loop transfer function from r to $e_{ms} = r - x_{ms}$, and $W_e = 0.5\pi/s$. This weight enforces $H_{r,e_{ms}}$ to be of system type 1, and minimizing γ_e corresponds to maximizing the bandwidth. Load tracking is quantified by $\gamma_d = \|H_{d_\theta,\theta}\|_\infty$, such that minimizing γ_d corresponds to maximizing the damping of f_n in $H_{d_\theta,\theta}$: the closed-loop transfer function from d_θ to θ. As a third specification in the controller design problem, a constraint on the actuator effort is added: $\|W_u H_{r,u}\|_\infty < 1$, where $H_{r,u}$ denotes the closed-loop transfer function from r to u and $W_u = s/(10\pi)$ to bound the derivative of u, which equals the cart acceleration.

To achieve satisfactory performance in load tracking and angle disturbance rejection under bounded actuator effort, the following control problem is solved:

$$\begin{aligned}
\underset{K\in\mathcal{S}_5,\gamma_e,\gamma_d}{\text{minimize}} \quad & \gamma_e + \beta\gamma_d && \text{(12a)}\\
\text{subject to} \quad & \|W_e H_{r,e_{ms}}\|_\infty < \gamma_e && \text{(12b)}\\
& \|H_{d_\theta,\theta}\|_\infty < \gamma_d && \text{(12c)}\\
& \|W_u H_{r,u}\|_\infty < 1 && \text{(12d)}
\end{aligned}$$

where β regulates the trade-off between the conflicting load tracking and angle disturbance rejection requirements. This problem is of the form (2), which is clarified by grouping all exogenous inputs and regulated outputs in w and z respectively:

$$w = \begin{bmatrix} r \\ d_\theta \end{bmatrix}\,, \quad z = \begin{bmatrix} W_e e_{ms} \\ \theta \\ W_u u \end{bmatrix}\,.$$

The notation used in (12) showing the considered input-output channel gives more sense in application, and hence it is used instead of explicitly labeling all control specifications by the index i as in (2). The control problem is solved in discrete time for four different length values. Prior to solving (12), the system and the weighting functions are discretized at a sample frequency of 60 Hz using the zero-order-hold transformation.

C. Interpolating the controllers

In this section the control design technique is used to design the gain-scheduled controllers for the rope length values. In order to do this, local controllers of order four are designed for four different system models corresponding to the values $L = 0.35, 0.45, 0.55, 0.75$. Next the described interpolation technique is used to derive the gain-scheduled controller for the whole range of the rope length variations.

Four MIMO controllers for local system models are derived considering the two degrees of freedom control configuration of Figure 3 and using the control design technique described in Section IV-B. The $\mathcal{H}_\infty$ norm of the function $H_{d_\theta,\theta}$ is a measure for disturbance rejection performance and hence the

appropriate value of β in (12) is adapted to keep $\|H_{d_\theta,\theta}\|_\infty \approx 16$ dB while the bandwidth is maximized. In this section different steps of the design are described.

1) In order to construct consistent SISO models, the second channel of the controllers (from the angle θ to the control signal u) is selected and transformed to a consistent SISO representation. To do this, two second order submodels each with two zeros are considered and the new representation is built as in (8).

2) Having these four consistent models, the transformation matrix that takes the original SISO controller $\widetilde{\mathsf{K}}_{\ell,(2,1)}$ to the consistent SISO controller $\mathsf{K}_{\ell,(2,1)}$ is calculated. This transformation matrix is then used to build the MIMO controller K_ℓ.

3) The consistent MIMO controllers are interpolated by solving the linear least square problem using a second order polynomial of L. Therefore any controller in this range of variation is calculated as:

$$K(L) = K_0 + LK_1 + L^2K_2 \tag{13}$$

The unknown variables K_0, K_1, K_2 are calculated by solving the least square problem of (10) which results in $\mathbf{E} = 0.09$. The following section discusses the validation of the gain-scheduled controller of (10) and shows that the performance specifications are met.

D. Validation of gain-scheduled controller

This sections discusses the validation of the gain-scheduled controller of (13) on the over-head crane. There exist different approaches to provide a stability certificate for the closed-loop system with time-varying parameters ([7], [8]). However, the validation of the gain-scheduled controller in this paper is based on extensive simulations with time-varying and time-invariant parameters.

In case of fixed length values, closed-loop frequency- and time-domain response are validated for 9 values of L equidistantly distributed in the interval $L = [0.35, 0.75]$ m. The performance is also validated by comparing local LTI controllers with the gain-scheduled controller through the closed-loop bandwidth and $\|H_{d_\theta,\theta}\|_\infty$. In case of varying length, the time-domain response of the system is evaluated for slow and fast parameter variation.

1) Fixed length validation: Figure 4 depicts the bode diagram of the functions considered in (12). By increasing the rope length from $L = 0.35$ m to $L = 0.75$ m, the colored lines vary from the most blue to the most red. In Figure 4(a), it is evident that the bandwidth decreases by increasing the rope length. As it is stated before, the norm $\|H_{d_\theta,\theta}\|_\infty \approx 16$ dB is kept fixed, which is shown in Figure 4(b).

The time-domain validation is based on closed-loop responses to a step input in r and an impulse input in d_θ for 9 considered rope length values. This is shown in Figure 5 for the same values of L. Tracing from blue to red, the step response gets slower and swinging of the mass gets larger. This results in more overshoot in step response. By the

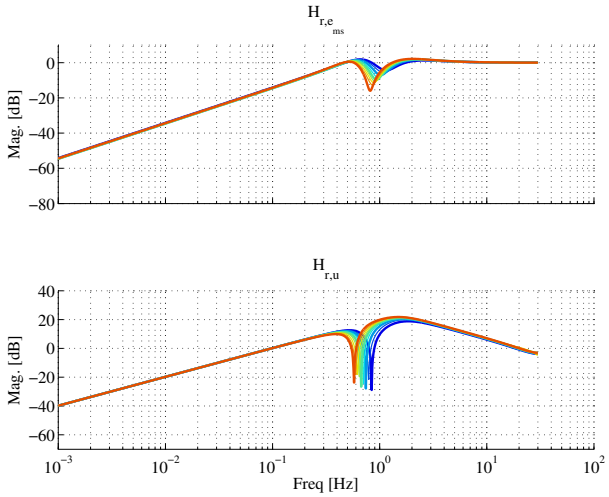

(a) From reference input

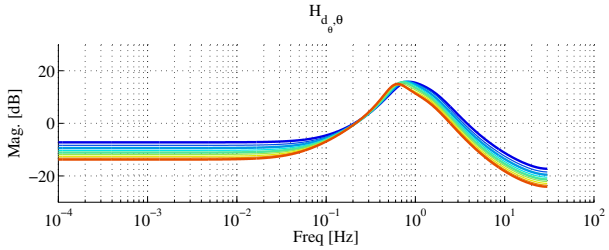

(b) From disturbance input

Fig. 4. Closed-loop frequency response by applying the gain-scheduled controller. The parameter L varies from 0.35 corresponding to the most blue line, to 0.75 the most red line, in (a), (b).

construction of d_θ, the impulse responses presented in Figure 5 correspond to the autonomous responses from an initial swing angle deviation. Since the norm $\|H_{d_\theta,\theta}\|_\infty$ is kept fixed, the settling times in impulse response are similar in the impulse response shown in Figure 5.

Figure 6 compares the bandwidth and the norm $\|H_{d_\theta,\theta}\|_\infty$ of two closed-loop systems as a function of L. One using the local LTI controllers and the other one using gain-scheduled controller evaluated at the considered 9 rope legth values. As it is mentioned before, the bandwidth decreases as the rope length increases and comparison shows that the gain-scheduled controller has a slightly lower bandwidth. The dots on the dashed-back line represent the local LTI controllers K_ℓ. Figure 6 also shows that the norm value with the gain-scheduled controller is slightly higher. The difference between the gain-scheduled and local LTI controller is due to the interpolation error and it is acceptable since the gain-scheduled controller gives satisfactory performance.

2) Varying length validation: A set of simulations with varying rope length have been performed and in this paper two representative results are shown: The step response with a length value varying from $L = 0.35$ to $L = 0.75$ at two different constant rates of $20m/sec$ and $0.08m/sec$. Figure 7 shows the step responses and rope length for fast and slow

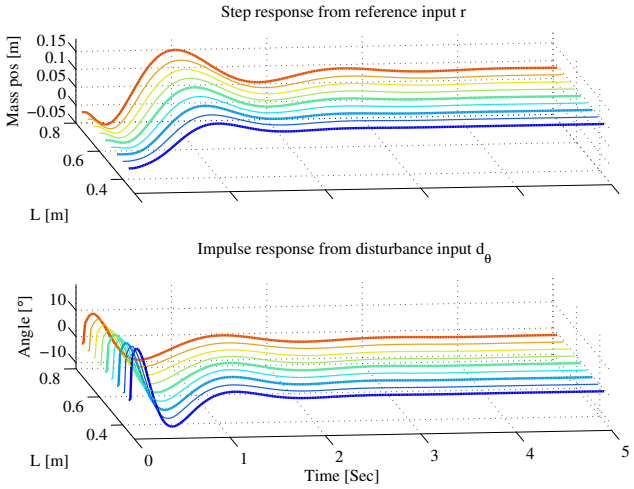

Fig. 5. Time response of the closed-loop system.

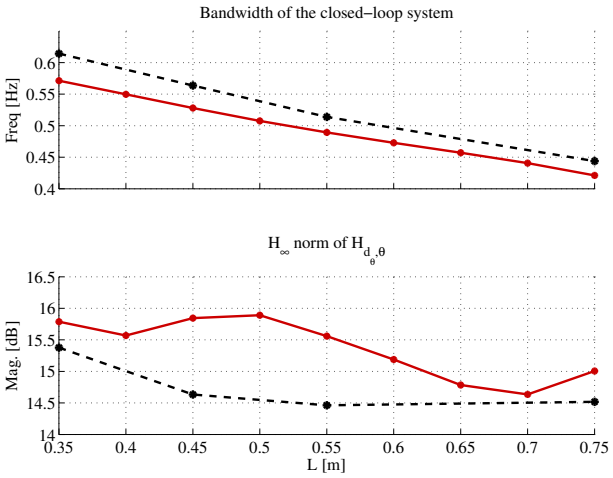

Fig. 6. Closed-loop bandwidth and $\|H_{d_\theta,\theta}\|_\infty$ as a function of L. Local LTI controllers (dashed-black) compared to the gain-scheduled controller (solid-red).

variation. The length change is applied at $t = 0.5$ sec while the step response is not settled and as we see the response gets more oscillatory but not unstable at fast length variations.

V. Conclusion

A practical method for designing gain-scheduled controllers for LPV systems is presented. A recently developed interpolation technique (SMILE) for modeling LPV systems is used to derive gain-scheduled controllers from local controllers. The local LTI control design is performed by splitting the classical $\mathcal{H}_\infty$ control problem into $\mathcal{H}_\infty$ constraints and objectives on selected closed-loop subsystems. The design approach is then applied to an over-head crane system with a varying rope length that should meet conflicting angle disturbance rejection and reference tracking performance requirements. These results reveal the value of our approach for LPV control.

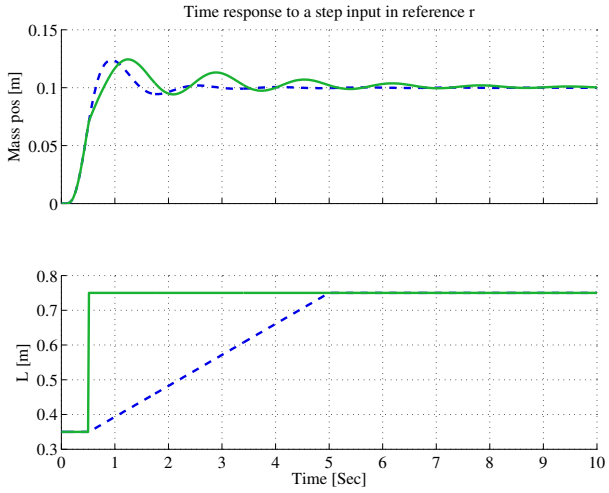

Fig. 7. Position of the load with parameter variation. Fast parameter variation (solid-green) and slow parameter variation (dashed-blue).

VI. Acknowledgement

Goele Pipeleers is a Postdoctoral Fellow of the Research Foundation Flanders (FWO Vlaanderen). This work benefits from K.U.Leuven BOF PFV/10/002 Center-of-Excellence Optimization in Engineering (OPTEC), the Belgian Programme on Interuniversity Attraction Poles, initiated by the Belgian Federal Science Policy Office (DYSCO), research projects G.0377.09 and G.0002.11 of the Research Foundation Flanders (FWO Vlaanderen), FP7- EMBOCON (ICT-248940), and K.U.Leuvens Concerted Research Action GOA/10/11 Global real-time optimal control of autonomous robots and mechatronic systems.

References

[1] D. J. Leith and W. E. Leithhead, "Survey of gain-scheduling analysis and design," *INT. J. CONTROL*, vol. 73, no. 11, pp. 1001 – 1025, 2000.

[2] D. C. J., C. J.F., P. B., and S. J., "An application of interpolating gain-scheduling control," in *Proc. third IFAC Symp. Syst., Struct. and Control*, Oct. 2007.

[3] J. De Caigny, J. Camino, and J. Swevers, "Interpolation-based modeling of MIMO LPV systems," *IEEE Transactions on Control Systems Technology*, vol. 19, no. 1, pp. 46 –63, Jan. 2011.

[4] K. Glover and J. C. Doyle, "State-space formulae for all stabilizing controllers that satisfy an $\mathcal{H}_\infty$-norm bound and relations to risk sensitivity," *Systems & Control Letters*, vol. 11, pp. 167–172, 1988.

[5] C. Scherer, P. Gahinet, and M. Chilali, "Multiobjective output-feedback control via lmi optimization," *IEEE Transactions on Automatic Control*, vol. 42, no. 7, pp. 896–911, 1997.

[6] I. Masubuchi, A. Ohara, and N. Suda, "A linear matrix inequality approach to $\mathcal{H}_\infty$ control," *LMI-based controller synthesis: A unified formulation and solution*, vol. 8, no. 8, pp. 669–686, 1998.

[7] F. Amato, M. Mattei, and A. Pironti, "Gain scheduled control for discrete-time systems depending on bounded rate parameters," *Int. J. Robust Nonlinear Control*, vol. 15, pp. 473–494, 2005.

[8] J. Daafouz and J. Bernussou, "Parameter dependent lyapunov functions for discrete time systems with time varying parametric uncertainties," *Systems & Control Letters*, vol. 43, no. 5, pp. 355–359, 2001.